**Atmospheric
Chemistry
and Physics**

Comprehensively accounting for the effect of giant CCN in cloud activation parameterizations

D. Barahona[1]**, R. E. L. West**[3]**, P. Stier**[3]**, S. Romakkaniemi**[4]**, H. Kokkola**[5]**, and A. Nenes**[1,2]

[1] School of Chemical and Biomolecular Engineering, Georgia Institute of Technology, USA
[2] School of Earth and Atmospheric Sciences, Georgia Institute of Technology, USA
[3] Atmospheric, Oceanic and Planetary Physics, Department of Physics, University of Oxford, UK
[4] Department of Physics and Mathematics, University of Eastern Finland, Finland
[5] Finnish Meteorological Institute, Kuopio Unit, Finland

Abstract. Large cloud condensation nuclei (CCN) (e.g., aged dust particles and seasalt) cannot attain their equilibrium size during the typical timescale of cloud droplet activation. Cloud activation parameterizations applied to aerosol with a large fraction of large CCN often do not account for this limitation adequately and can give biased predictions of cloud droplet number concentration (CDNC). Here we present a simple approach to address this problem that can easily be incorporated into cloud activation parameterizations. This method is demonstrated with activation parameterizations based on the "population splitting" concept of Nenes and Seinfeld (2003); it is shown that accounting for large CCN effects eliminates a positive bias in CDNC where the aerosol dry geometric diameter is greater than 0.5 µm. The method proposed here can also be extended to include the water vapor depletion from pre-existing droplets and ice crystals in global and regional atmospheric models.

1 Introduction

Cloud droplet activation is the direct microphysical link between aerosol and clouds, and its accurate description is essential for studying aerosol indirect climate effects. Sophisticated parameterizations are currently used for describing activation in global circulation models, based on solutions to the coupled mass and energy balance for a Lagrangian cloud parcel (e.g., Abdul-Razzak and Ghan, 2000; Cohard et al., 2000; Nenes and Seinfeld, 2003; Fountoukis and Nenes, 2005; Ming et al., 2006). Depending on the formulation, effects of the aerosol composition (e.g., Abdul-Razzak and Ghan, 2000; Fountoukis and Nenes, 2005), adsorption activation (Kumar et al., 2009), mixing and entrainment (Barahona and Nenes, 2007), and mass transfer limitations on droplet growth (Fountoukis and Nenes, 2005; Ming et al., 2006) can explicitly be accounted for.

In accordance with Köhler theory, cloud condensation nuclei (CCN) activate into cloud droplets when the ambient supersaturation is above the global maximum of their equilibrium curve (termed "critical supersaturation") and sufficient time is allowed for their wet size to exceed their critical diameter (Seinfeld and Pandis, 1998). Most often, the timescale of equilibration of CCN (up to the point of activation) is shorter than the rate of change of supersaturation in ambient clouds; this gives rise to the assumption that CCN instantaneously equilibrate with their environment. However, droplet growth may be subject to a variety of kinetic limitations, one of which is the so-called "inertial mechanism" (Nenes et al., 2001). Due to their large dry size, inertially-limited particles, although having very low critical supersaturation, cannot attain their critical size within the timescale typically associated with activation in clouds. Despite this, such particles are comparable in size to strictly activated droplets and can still contribute substantial amounts of liquid water content (LWC) and surface area, particularly in polluted clouds where the supersaturation is very low (Charlson et al., 2001). Therefore, assuming that all droplets exceed their equilibrium size at the point of maximum supersaturation tends to overestimate

their liquid water content and surface area (Chuang et al., 1997; Nenes et al., 2001); parameterizations that neglect these kinetic limitations underestimate cloud droplet number concentration (CDNC) (Phinney et al., 2003).

Including the contribution of inertially-limited CCN in cloud droplet activation parameterizations is not trivial. Ming et al. (2006) proposed the usage of a semi-empirical power law to express growth; although effective, its application in existing parameterization frameworks may not be straightforward. Nenes and Seinfeld (2003) used the concept of "population splitting" to differentiate between particles that activate and those that are inertially-limited. The approach of Twomey (1959) is used for the latter, which works for most atmospheric aerosol and presumes the size of droplets at cloud base is negligible compared to the growth experienced up to the level of maximum supersaturation in the cloud (e.g., Twomey, 1959; Nenes and Seinfeld, 2003). This assumption is subject to increasingly-large error as the dry particle size increases and can lead to significant underestimation in droplet size and surface area if giant CCN are present. Under such conditions, the condensation rate of water vapor is underestimated, which leads to overestimation in maximum supersaturation, s_{max}, and droplet number (e.g., Barahona and Nenes, 2007; Kumar et al., 2008).

This work proposes a new approach to account for the contribution of initially-limited CCN to the condensation surface area in the water vapor balance equations. The application of this method does not require reformulation of a parameterization, and is illustrated using the parameterizations of Nenes and Seinfeld (2003) and Fountoukis and Nenes (2005).

2 Development of inertial effect correction

Every physically-based droplet formation parameterization conceptually consists of two steps, one involving the determination of the "CCN spectrum" (i.e., the number of CCN that can activate at a given level of supersaturation computed by e.g., Köhler or adsorption activation theory) and one determining the maximum supersaturation, s_{max}, that develops in the ascending parcel. The droplet number concentration is then just the value of the CCN spectrum at s_{max}. The supersaturation in the ascending parcel is determined from (Seinfeld and Pandis, 1998; Nenes and Seinfeld, 2003; Barahona and Nenes, 2007),

$$\frac{ds}{dt} = \alpha V \left(1 - \frac{e}{e_c}\right) - \gamma \frac{dW}{dt} \tag{1}$$

where $\frac{dW}{dt}$ is the rate of condensation of liquid water onto the drops, V is the updraft velocity, $\alpha = \frac{gM_w\Delta H_v}{c_pRT^2} - \frac{gM_a}{RT}$, $\gamma = \frac{pM_a}{p^s(T)M_w} + \frac{M_w\Delta H_v^2}{c_pRT^2}$, ΔH_v is the latent heat of vaporization of water, g is the acceleration due to gravity, T and T' are the parcel and ambient temperature, respectively, c_p is the

heat capacity of air, $p^s(T)$ is the water saturation vapor pressure (over a flat surface) at T, p is the ambient pressure, M_w and M_a are the molar masses of water and air, respectively, and R is the universal gas constant. Homogeneous mixing of dry air is accounted for by using a fractional entrainment rate, e, (for an adiabatic parcel, mixing effects are negligible, i.e., $e = 0$); $e_c \approx \alpha \left[(1 - \text{RH}) - \frac{\Delta H_v M_w}{RT^2}(T - T')\right]^{-1}$, is the critical entrainment rate at which supersaturation is no longer generated in the parcel (Barahona and Nenes, 2007) and RH is the ambient relative humidity. The maximum supersaturation, s_{max}, is found from Eq. (1) by setting $\frac{ds}{dt} = 0$.

When large CCN are not contributing to droplet number, $\frac{dW}{dt}$ at the point of maximum supersaturation in the cloud ascent is denoted as $\frac{dW}{dt}\big|_{ps}$, and computed using the parameterization of interest. When inertially-limited CCN dominate $\frac{dW}{dt}$, then droplets do not substantially change size from cloud base to the level of s_{max}; the condensation rate in this limit is denoted as $\frac{dW}{dt}\big|_{ie}$. When both activated and inertially-limited CCN contribute to condensation, $\frac{dW}{dt}$ at the point of maximum supersaturation can be written as

$$\frac{dW}{dt} = \frac{dW}{dt}\bigg|_{ie} + \frac{dW}{dt}\bigg|_{ps} \tag{2}$$

$\frac{dW}{dt}\big|_{ie}$ can be computed from the liquid water content at cloud base in equilibrium with the aerosol particles that would eventually become droplets, i.e.,

$$W|_{ie} = \frac{\pi}{6}\frac{\rho_w}{\rho_a}\left[\int_{\ln D_{p\min}}^{\infty} D_p^3 n(\ln D_p)d\ln D_p\right] \tag{3}$$

where $n(D_p)$ is the droplet size distribution, and D_p is their size at saturation. If the aerosol is assumed to follow classical Köhler theory, D_p can be shown to be,

$$D_p = \frac{2}{3\sqrt{3}}\frac{A}{s_c} \tag{4}$$

where $A = \frac{4\sigma M_w}{RT\rho_w}$, σ is the surface tension of the droplet at saturation, and s_c is the droplet critical supersaturation. $D_{p\min}$ in Eq. (3) is the equilibrium diameter, at saturation, of the smallest particle that activates (i.e., for which $s_c = s_{max}$), i.e., $D_{p\min} = \frac{2}{3\sqrt{3}}\frac{A}{s_{max}}$.

$\frac{dW}{dt}\big|_{ie}$ is calculated taking the time derivative of Eq. (3), assuming that the droplet growth rate is given by $\frac{dD_p}{dt} = \frac{Gs}{D_p}$ (e.g., Nenes and Seinfeld, 2003) and the diameter does not change between cloud base and s_{max},

$$\frac{dW}{dt}\bigg|_{ie} = \frac{\pi}{2}\frac{\rho_w}{\rho_a}Gs\left[\int_{\ln D_{p\min}}^{\infty} D_p n(\ln D_p)d\ln D_p\right] \tag{5}$$

with

$$G = \frac{4}{\frac{\rho_w RT}{p^s(T)D_v'M_w} + \frac{\Delta H_v \rho_w}{k_a T}\left(\frac{\Delta H_v M_w}{RT} - 1\right)} \tag{6}$$

where k_a is the thermal conductivity of air, and D'_v is the water vapor mass transfer coefficient from the gas to droplet phase corrected for non-continuum effects, computed as suggested by Fountoukis and Nenes (2005).

2.1 Calculating the wet size distribution of inertially-limited CCN

Expressing the critical supersaturation in terms of the dry aerosol properties, Eq. (4) can be expressed in terms of the dry size, d_s, as

$$D_p = \left(\frac{B}{A}\right)^{1/2} d_s^{3/2} \tag{7}$$

where $B = \frac{\varepsilon_s \nu M_w}{M_s \rho_w}\left(\frac{\varepsilon_s}{\rho_s} + \frac{1-\varepsilon_s}{\rho_u}\right)^{-1}$, ν is the effective van't Hoff factor, ε_s is the mass fraction of soluble material, and ρ_s and ρ_u are the densities of the soluble and insoluble fractions of the dry particle, respectively. Using Eq. (7), the wet size distribution at saturation can be expressed in terms of the dry size distribution as

$$n(\ln D_p) = \frac{dN_d}{d\ln D_p} = \frac{dN_d}{d\ln d_s}\frac{d\ln d_s}{d\ln D_p} = \frac{2}{3}\frac{dN_d}{d\ln d_s} \tag{8}$$

where $N_d = \int\limits_{D_{p,\min}}^{\infty} n(D_p)dD_p$ is the droplet number concentration.

For a lognormal aerosol representation,

$$\frac{dN_a}{d\ln d_s} = \sum_{i=1}^{n_m}\frac{N_i}{\sqrt{2\pi}\ln\sigma_i}\exp\left[-\frac{\ln^2\left(d_s/d_{g,i}\right)}{2\ln^2\sigma_i}\right] \tag{9}$$

where $d_{g,i}$, σ_i are the geometric mean diameter and standard deviation of mode i, respectively, n_m is the number of log-normal modes, N_a the total aerosol concentration, and N_i is the aerosol concentration of mode i. Substituting Eqs. (7) and (8) into Eq. (9) gives

$$\frac{dN_d}{d\ln D_p} = \sum_{i=1}^{n_m}\frac{2}{3}\frac{N_i}{\sqrt{2\pi}\ln\sigma_i}\exp\left[-\frac{4}{9}\frac{\ln^2\left(D_p/D_{g,i}\right)}{2\ln^2\sigma_i}\right] \tag{10}$$

where $D_{g,i}$ is the equilibrium size of $d_{g,i}$ at saturation given by Eq. (7). Substitution of Eq. (10) into Eq. (5) gives the condensation rate of inertially-limited CCN at $s_{\max}$,

$$\left.\frac{dW}{dt}\right|_{ie} = \frac{\pi}{2}\frac{\rho_w}{\rho_a}Gs_{\max}\sum_{i=1}^{n_m}\frac{N_i}{2}D_{g,i}\exp\left(\frac{9}{8}\ln^2\sigma_i\right)$$
$$\text{erfc}\left[\frac{2}{3\sqrt{2}}\frac{\ln(D_{p\min}/D_{g,i})}{\ln\sigma_i} - \frac{3}{2\sqrt{2}}\ln\sigma_i\right] \tag{11}$$

Alternatively, Eq. (11) can be written in terms of the mean droplet diameter, $\bar{D}_p = \frac{1}{N_d}\int\limits_{\ln D_{p\min}}^{\infty} D_p n(\ln D_p)d\ln D_p$, as

$$\left.\frac{dW}{dt}\right|_{ie} = \frac{\pi}{2}\frac{\rho_w}{\rho_a}Gs_{\max}N_d\bar{D}_p. \tag{12}$$

For a sectional aerosol representation,

$$\frac{dN_a}{d\ln d_s} \cong \frac{\Delta N_m}{\Delta\ln d_{s,m}} = \frac{\Delta N_m}{\ln d_{s,m} - \ln d_{s,m-1}} \tag{13}$$

where ΔN_m is the number concentration of particles in section m, and, $d_{s,m}$ and $d_{s,m-1}$ are the "upper" and "lower" dry diameters of the section m, respectively (Nenes and Seinfeld, 2003). Substituting Eqs. (7) and (8) into Eq. (13) gives

$$\frac{dN_d}{d\ln D_p} \cong \frac{\Delta N_m}{\Delta\ln D_{p,m}} = \frac{\Delta N_m}{\ln D_{p,m} - \ln D_{p,m-1}} \tag{14}$$

where $D_{p,m}$ and $D_{p,m-1}$ are the droplet diameters in equilibrium with $d_{s,m}$ and $d_{s,m-1}$, respectively. Substitution of Eq. (14) into Eq. (5) gives,

$$\left.\frac{dW}{dt}\right|_{ie} = \frac{\pi}{2}\frac{\rho_w}{\rho_a}Gs_{\max}\sum_{m=i_{\max}}^{n_{\text{sec}}}D_{p,m}\frac{\Delta N_m}{\Delta\ln D_{p,m}}\Delta\ln D_{p,m} \tag{15}$$

where n_{sec} is the total number of sections and $D_{p,m}$ is averaged within section m, and $i_{\max}$ is the section that contains $s_{\max}$. Defining the average droplet diameter at the limit where all are kinetically limited as $\bar{D}_p = \frac{1}{N_d}\sum\limits_{m=i_{\max}}^{n_{\text{sec}}}D_{p,m}\frac{\Delta N_m}{\Delta\ln D_{p,m}}\Delta\ln D_{p,m}$, the condensation rate $\left.\frac{dW}{dt}\right|_{ie}$ for sectional aerosol can also be expressed in the form of Eq. (12).

3 Implementing inertially-limited CCN effects: demonstration for "population splitting" activation frameworks

Using the "population splitting" approach of Nenes and Seinfeld (2003), $\left.\frac{dW}{dt}\right|_{ps}$ at $s_{\max}$ can be written as the sum of two terms,

$$\left.\frac{dW}{dt}\right|_{ps} = \frac{\pi}{2}\frac{\rho_w}{\rho_a}Gs_{\max}\left[I_1(0,s_{\text{part}}) + I_2(s_{\text{part}},s_{\max})\right] \tag{16}$$

The functions $I_1(0,s_{\text{part}})$ and $I_2(s_{\text{part}},s_{\max})$ are given in Nenes and Seinfeld (2003) (hereafter NS03) and Fountoukis and Nenes (2005) for sectional and lognormal aerosol representations, respectively. The partition supersaturation, s_{part}, separates two CCN populations, one (expressed by I_2) for which droplets experience negligible growth beyond the critical diameter ($s_c \approx s_{\max}$), and one (expressed as I_1) for which droplet growth is much larger than the critical diameter ($s_c \ll s_{\max}$). In reality, the large kinetically-limited CCN compose a third population, as they have low s_c, but do not reach their critical diameter at the point of $s_{\max}$. Nenes and Seinfeld (2003) recognized this, and postulated (guided by numerical simulations) that the growth experienced by these particles is still substantially larger than their dry diameter, hence can be approximated with I_1. This approximation may not apply for very large and giant CCN; as suggested by
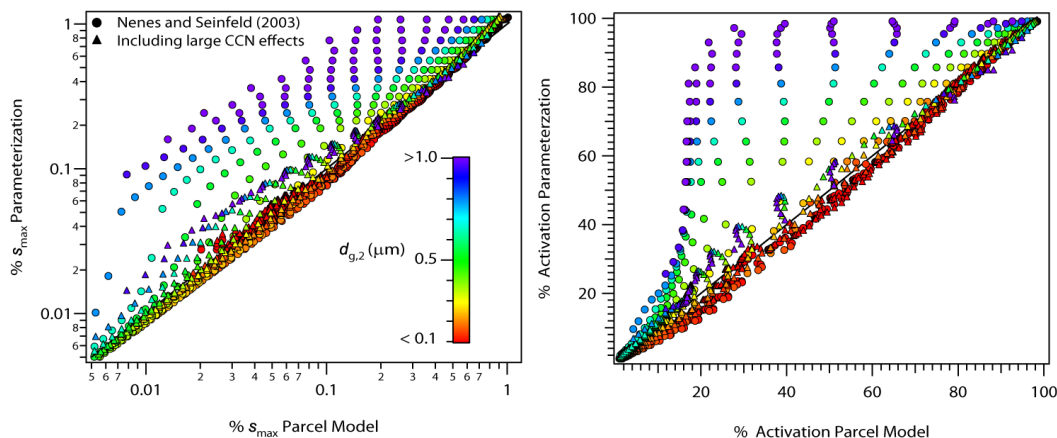
Fig. 1. Maximum supersaturation (left) and aerosol activation fraction (right) for a bimodal aerosol distribution. Results are from application of the Nenes and Seinfeld (2003) parameterization neglecting (circles) and considering (triangles) the effect of kinetic limitations on large CCN. Conditions considered are $N_1 = 2000\,\text{cm}^{-3}$ and $N_2 = 400\,\text{cm}^{-3}$, $\sigma_1 = \sigma_2 = 1.59$, $d_{g,1} = 0.08\,\mu\text{m}$, $T = 290\,\text{K}$, $p = 100\,\text{kPa}$, and $\alpha_c = 0.06$. Color coding varies with the geometric mean diameter of the coarse mode. Symbols within the same color vary with updraft speed.

Eq. (2), a third term, $\left.\frac{dW}{dt}\right|_{ie}$, must be added to Eq. (16) to account for their effect on the condensation rate.

Combining Eqs. (16), (2), and Eq. (12) gives for the supersaturation balance at s_{max},

$$\frac{\frac{\pi}{2}\frac{\rho_w}{\rho_a} G s_{\text{max}}}{\frac{\alpha V}{\gamma}\left(1 - \frac{e}{e_c}\right)}\left\{ I_1(0, s_{\text{part}}) + I_2(s_{\text{part}}, s_{\text{max}}) + N_a\,\bar{D}_p\big|_{s_{\text{part}}} \right\} - 1 = 0 \quad (17)$$

$\bar{D}_p\big|_{s_{\text{part}}}$ is calculated at s_{part} instead of s_{max} (i.e., $D_{p\,\text{min}} = \frac{2}{3\sqrt{3}}\frac{A}{s_{\text{part}}}$ in Eqs. 11 and 15). This is justified as s_{part} represents the limit between particles that experienced significant growth after activation and those that are kinetically limited (Nenes and Seinfeld, 2003). Equation (17) constitutes the extension of the population-splitting droplet activation parameterization to include the inertially-limited CCN effects. It is solved iteratively to find s_{max}; cloud droplet number concentration is then calculated from the cumulative CCN spectrum, $F^s(s)$, at s_{max} (Nenes and Seinfeld, 2003).

## 4 Comparison against parcel model results

The modified population-splitting activation parameterization is evaluated by comparing predictions of s_{max} and droplet number against simulations with a comprehensive cloud parcel model (Nenes et al., 2001) for a wide range of updraft velocities and aerosol size distribution characteristics. Initial parcel temperature and pressure were 290 K and 100 kPa, respectively, and the water uptake coefficient was set to 0.06, following the suggestions of Fountoukis et al. (2007). All aerosol particles are assumed to be initially in equilibrium with the surrounding environment at RH=80%. Consistent with other studies (e.g., Phinney et al., 2003), using a higher initial RH would result in slightly lower

CDNC (mostly within 10%) for updraft velocities lower than $0.1\,\text{m s}^{-1}$. However, varying the initial RH between 60 and 90% causes little CDNC variability (not shown).

Entrainment reduces supersaturation generation from expansion cooling and reduces s_{max}. Given the wide range of s_{max} seen in the simulations (from the variation in V and aerosol characteristics) varying e is unnecessary; we therefore set $e=0$ in all simulations presented. After s_{max} is reached, entrainment effects may substantially modify the droplet size distribution (e.g., Pruppacher and Lee, 1976; Lin and Arakawa, 1997; Su et al., 1998) but these are beyond the scope of this work.

The aerosol is assumed to be pure ammonium sulfate and composed of two lognormal modes, with number concentration $N_1 = 2000\,\text{cm}^{-3}$ and $N_2 = 400\,\text{cm}^{-3}$, respectively. The geometric dispersion for both modes is set to $\sigma_1 = \sigma_2 = 1.59$; $d_{g,1}$ is set to $0.08\,\mu\text{m}$. These values were selected as representative of atmospheric aerosol (Seinfeld and Pandis, 1998); Sect. 4.1 presents sensitivity runs using different sets of parameters. V was varied over conditions expected in GCM simulations (0.01 to $10\,\text{m s}^{-1}$), and $d_{g,2}$ was varied between 0.005 and $5\,\mu\text{m}$ to represent typical values of recently nucleated particles ($<0.01\,\mu\text{m}$) and/or giant CCN ($>1\,\mu\text{m}$) (Pruppacher and Klett, 1997).

Parcel model results indicate that at high $V (> 5\,\text{m s}^{-1})$ and moderate $d_{g,2}$ (less than $0.1\,\mu\text{m}$) the activation fraction reaches high values as the s_{max} is sufficient ($\sim 1\%$) to activate most CCN. As $d_{g,2}$ increases, significant water vapor depletion by droplets in the coarse mode decreases s_{max}, therefore reducing the activation fraction (mostly in the fine mode). As $d_{g,2}$ becomes substantially large ($>0.5\,\mu\text{m}$), the activation fraction approaches 16% (i.e., $N_1/(N_1 + N_2)$) as all particles in the coarse mode are activated (i.e., they have $s_c < s_{\text{max}}$) but virtually none in the fine mode. At this limit,
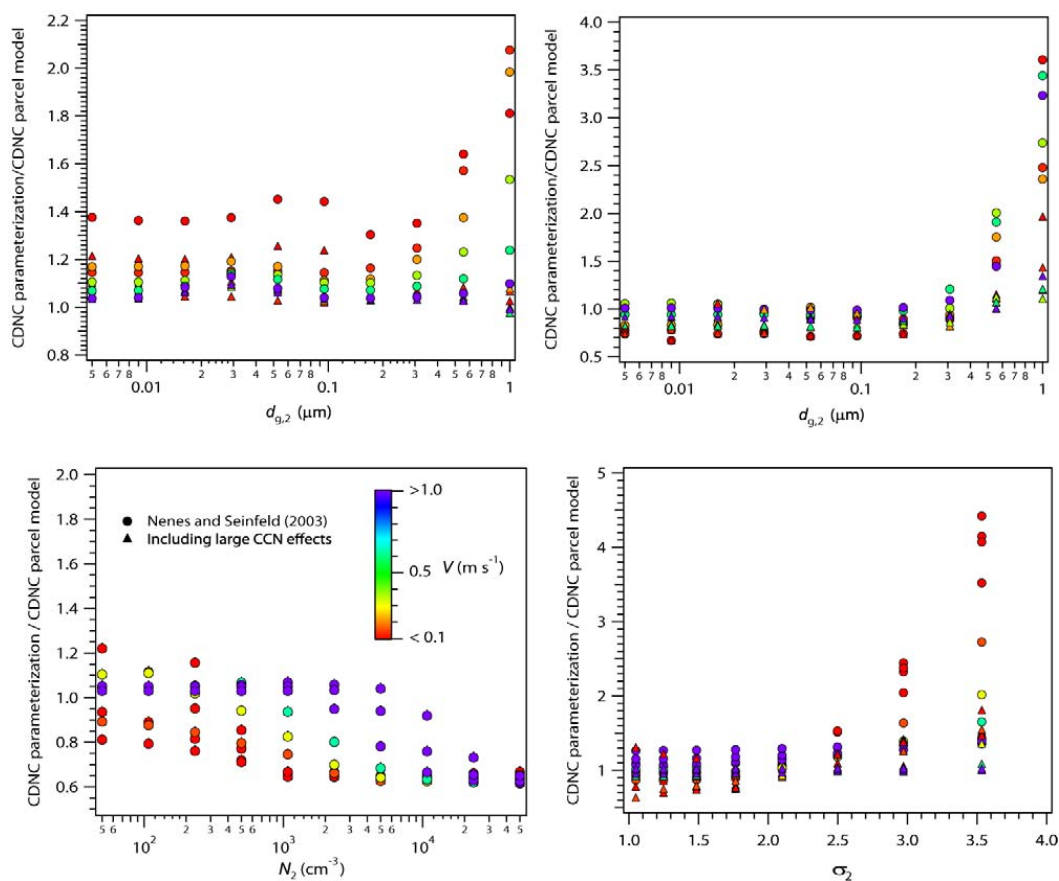
Fig. 2. CDNC predicted by the parameterization over CDNC predicted by the parcel model as a function of the geometric mean diameter (top panels), aerosol number concentration (bottom left panel) and the geometric dispersion (bottom right panel) of the coarse mode, for a bimodal aerosol distribution. Simulations were performed for $N_1 = 100 \, \text{cm}^{-3}$ and $N_2 = 50 \, \text{cm}^{-3}$ (top, left panel), $\varepsilon_s = 0.4$ (top, right panel), $d_{g,2} = 0.12 \, \mu\text{m}$, $\sigma_1 = \sigma_2 = 1.59$ (bottom, left panel), $d_{g,1} = 0.08 \, \mu\text{m}$, $d_{g,2} = 0.12 \, \mu\text{m}$, $\sigma_1 = 1.59$ (bottom, left panel). All other conditions are similar to Fig. 1. Color coding varies with updraft speed.

underestimating the surface area from large CCN overpredicts s_{max} and the activation fraction hence the droplet concentration, especially for $d_{g,2} > 0.5 \, \mu\text{m}$ (Fig. 1). This is in agreement with the results of Phinney et al. (2003) who showed that neglecting the effect of inertially-limited particles would result in an overestimation in CDNC (as opposed to assuming equilibrium conditions which results in underestimation of CDNC). Accounting for depletion effects from inertially-limited CCN largely corrects this bias (Eq. 17) producing results that are in agreement with the parcel model. Figure 1 shows that for $d_{g,2} > 0.5 \, \mu\text{m}$, significant deviations between the parameterization and the parcel model occur (depicted by circles); which are to a large extent reduced at lower $d_{g,2}$. Application of the large CCN correction for $d_{g,2} > 0.5 \, \mu\text{m}$ significantly reduces the difference in s_{max} between the parameterization and the parcel model (triangles).

4.1 Sensitivity tests

The sensitivity of the parameterization results to N_1, N_2, σ_2, and the aerosol soluble fraction, ε_s, is presented in Fig. 2. Repeating the simulations of Fig. 1 for "clean" conditions, i.e., $N_1 = 100 \, \text{cm}^{-3}$ and $N_2 = 50 \, \text{cm}^{-3}$ (Fig. 2, top left panel), tests the robustness of the large CCN correction to aerosol number concentration. NS03 tends to slightly overestimate CDNC (Nenes and Seinfeld, 2003; Barahona and Nenes, 2007), particularly at low V ($< 0.1 \, \text{m s}^{-1}$, hence low activation fractions); the overestimation being larger for $d_{g,2} > 0.5 \, \mu\text{m}$. Including the effects of large CCN corrects this and CDNC remains mostly within a 10% of the parcel model results.

The sensitivity of CDNC predictions to aerosol composition was assessed by reducing the coarse mode sulfate fraction to 0.4 (Fig. 2, top right panel). CDNC predicted by NS03 is within 20% from the parcel model results (with a slightly higher underestimation for $V < 0.1 \, \text{m s}^{-1}$); for

$d_{g,2} > 0.5\,\mu m$, NS03 largely overpredicts CDNC. Including large CCN effects corrects this, however, significant overprediction ($>50\%$) may still result for $d_{g,2} > 1\,\mu m$ and $V \sim 0.1\,m\,s^{-1}$, which results from neglecting the contribution of the insoluble core to the saturated wet size, D_p, in Eq. (7). Using a modified version of Köhler theory (Khvorostyanov and Curry, 2007) can account for this issue.

Sensitivity tests were carried out for $d_{g,2} = 0.12\,\mu m$, and varying N_2 between 50 and $5 \times 10^4\,cm^{-3}$ (all other conditions similar to Fig. 1). At low $N_2 \sim 100\,cm^{-3}$, an increase in the activation fraction from 10% to 80% was produced when V increased from 0.1 to $1\,m\,s^{-1}$ (not shown); at high $N_2 > 10^4\,cm^{-3}$, significant activation fractions were found only for $V > 0.5\,m\,s^{-1}$. At these conditions, however, the effect of large CCN was not significant and the NS03 parameterization reproduced the results of the parcel model with a slight underprediction for $N_2 > 1000\,cm^{-3}$. Therefore the effect of giant CCN is expected to be negligible, as the surface area of the aerosol particles at cloud base is negligible compared to the surface area of activated droplets; thus significant droplet growth after activation occurs, and the equilibrium size at cloud base is negligible compared to the size after activation. Indeed, no change in CDNC is seen when the inertial correction is included (Fig. 2, bottom left panel).

A final sensitivity test was carried out for $d_{g,2} = 0.12\,\mu m$, $N_2 = 400\,cm^{-3}$ and varying σ_2 between 1.05 and 3.5 (all other conditions similar to Fig. 1). Including the effect of kinetically-limited CCN for $\sigma_2 > 2.5$ significantly reduces the activated fraction (Fig. 2, bottom right panel) (since a substantial fraction of aerosol are giant CCN) and the predicted CDNC shows good agreement with parcel model results. In all sensitivity tests, the effects of kinetically-limited CCN were much more pronounced when $d_{g,2}$ was increased to values over $0.5\,\mu m$, which is also evident in Fig. 1.

The CDNC assessment was repeated for the lognormal aerosol activation parameterization of Fountoukis and Nenes (2005), using Eq. (11) to calculate $\bar{D}_p\big|_{s_{part}}$; the calculated activated fraction was within 1% of the results using the sectional formulation of Nenes and Seinfeld (2003). Finally, for all the runs carried out in this study, including the correction for kinetically-limited CCN had a minor impact on computational time (2% and 7% increase for the sectional and lognormal versions of the parameterization, respectively).

5 Conclusions

When a significant fraction of large CCN are present during cloud formation (i.e., droplets which at the point of maximum supersaturation in a cloud updraft have not experienced significant growth compared to cloud base), their contribution to the droplet surface area must correctly be accounted for in parameterizations to avoid biases in maximum supersaturation and droplet number. A general correction is proposed for droplet activation parameterizations, where the condensation upon inertially-limited droplets is added to the "default" expression in the parameterization of interest. The correction was incorporated into the Nenes and Seinfeld (2003) and Fountoukis and Nenes (2005) parameterizations and tested for a wide range of conditions. Results show that incorporation of the correction greatly improved the parameterization performance for conditions where inertially-limited CCN dominate droplet formation, without significant impact on the computational burden of the parameterization. The approach outlined here can easily be extended to include adsorption activation of mineral dust (Kumar et al., 2009). It can also be applied to account for the water vapor depletion from pre-existing droplets and ice crystals during secondary activation events in convective updrafts, by appropriately modifying the growth constant and size distribution in Eq. (12) (e.g., Barahona and Nenes, 2009). The approach outlined here is a simple way to account for some of the prediction biases in regions strongly influenced by dust (e.g., Prospero and Lamb, 2003) and large sea salt particles (e.g., O'Dowd et al., 1997).

References

Abdul-Razzak, H. and Ghan, S.: A parameterization of aerosol activation, 2. Multiple aerosol types, J. Geophys. Res., 105, 6837–6844, doi:10.1029/1999JD901161, 2000.

Barahona, D. and Nenes, A.: Parameterization of cloud droplet formation in large scale models: including effects of entrainment, J. Geophys. Res., 112, D16026, doi:10.1029/16207JD008473, 2007.

Barahona, D. and Nenes, A.: Parameterizing the competition between homogeneous and heterogeneous freezing in ice cloud formation –polydisperse ice nuclei, Atmos. Chem. Phys., 9, 5933–5948, 2009,
http://www.atmos-chem-phys.net/9/5933/2009/.

Charlson, R. J., Seinfeld, J. H., Nenes, A., Kulmala, M., Laaksonen, A., and Facchini, M. C.: Reshaping the theory of cloud formation, Science, 292, 2025–2026, 2001.

Chuang, P. Y., Charlson, R. J., and Seinfeld, J. H.: Kinetic limitations on droplet formation in clouds, Nature, 390, 594–596, 1997.

Cohard, J.-M., Pinty, J.-P., and Suhre, K.: On the parameterization of activation spectra from cloud condensation nuclei microphysical properties, J. Geophys. Res., 105, 11753–11766, doi:10.1029/11999JD901195, 2000.

Fountoukis, C. and Nenes, A.: Continued development of a cloud droplet formation parameterization for global climate models, J. Geophys. Res., 110, D11212, doi:10.1029/12004JD005591, 2005.

Khvorostyanov, V. I. and Curry, J. A.: Refinements to the Köhler's theory of aerosol equilibrium radii, size spectra, and droplet activation: Effects of humidity and insoluble fraction, J. Geophys. Res., 112, D05206, doi:10.1029/02006JD007672, 2007.

Kumar, P., Sokolik, I. N., and Nenes, A.: Parameterization of cloud droplet formation for global and regional models: including adsorption activation from insoluble CCN, Atmos. Chem. Phys., 9, 2517–2532, 2009,
http://www.atmos-chem-phys.net/9/2517/2009/.

Lin, C. and Arakawa, A.: The macroscopic entrainment processes of simulated cumulus ensemble, Part II: Testing the entraining-plume model, J. Atmos. Sci., 54, 1044–1053, 1997.

Ming, Y., Ramaswamy, V., Donner, L. J., and Phillips, V. T. J.: A new parameterization of cloud droplet activation applicable to general circulation models, J. Atmos. Sci., 63, 1348–1356, 2006.

Nenes, A., Ghan, S., Abdul-Razzak, H., Chuang, P. Y., and Seinfeld, J. H.: Kinetic limitations on cloud droplet formation and impact on cloud albedo, Tellus, 53B, 133–149, 2001.

Nenes, A. and Seinfeld, J. H.: Parameterization of cloud droplet formation in global climate models, J. Geophys. Res., 108, 4415, doi:10.1029/2002JD002911, 2003.

O'Dowd, C. D., Smith, M. H., Consterdine, I. E., and Lowe, J. A.: Marine aerosol, sea-salt, and the marine sulphur cycle: A short review, Atmos. Environ., 31, 73–80, 1997.

Phinney, L. A., Lohmann, U., and Leaitch, W. R.: Limitations of using an equilibrium approximation in an aerosol activation parameterization, J. Geophys. Res., 108, 4371, doi:10.1029/2002JD002391, 2003.

Prospero, J. M. and Lamb, D.: African Droughts and Dust Transport to the Caribbean: Climate Change Implications, Science, 302, 1024–1027, 2003.

Pruppacher, H. R. and Lee, I.: A comparative study of the growth of cloud drops by condensation using an air parcel model with and without entrainment, Pure Appl. Geophys., 115, 523–545, 1976.

Pruppacher, H. R. and Klett, J. D.: Microphysics of clouds and precipitation 2nd ed., Kluwer Academic Publishers, Boston, MA 954 pp., 1997.

Seinfeld, J. H. and Pandis, S. N.: Atmospheric Chemistry and Physics, John Wiley and Sons, New York, NY, USA, 1998.

Su, C., Krueger, S. K., McMurtry, P. A., and Austin, P. H.: Linear eddy modeling of droplet spectral evolution during entrainment and mixing in cumulus clouds, Atmos. Res., 47–78, 41–58, 1998.

Twomey, S.: The nuclei of natural cloud formation, II. The supersaturation in natural clouds and the variation of cloud droplet number concentration, Pure Appl. Geophys., 43, 243–249, doi:210.1007/BF01993560, 1959.